

Impact of higher-order surface imperfections on the stiffness of flexure hinges

Martin Wittke, Maria-Theresia Ettelt, Matthias Wolf, Mario André Torres Melgarejo, Maximilian Darnieder, René Theska

Technische Universität Ilmenau, Department of Mechanical Engineering, Institute for Design and Precision Engineering, Precision Engineering Group

E-Mail: martin.wittke@tu-ilmenau.de

Abstract

Compliant mechanisms composed of stiff links and concentrated compliances are frequently used in high-precision force metrology. Low bending stiffness and minimum parasitic motions are often desired. Since the elasto-kinematic behavior of these systems is predominantly defined by the flexure hinges, they are implemented with high aspect ratios and minimum thicknesses down to about 50 μm . An unexpectedly strong deviation of the elasto-mechanic behavior of manufactured prototypes compared to the theoretical models was found. First investigations in the state of the art show that even minor deviations from the ideal hinge geometry can lead to a significant change in the properties. For first-order form deviations, the hinge thickness has been identified as the main impact factor. However, second and higher-order form deviations can also lead to a non-negligible thickness change in the flexure hinges significant region, but have not been investigated.

For this reason, this work deals with the impact of the waviness and periodic roughness on the stiffness of a semi-circular flexure hinge. Modeling and simulation of the hinges with a sinusoidal notch surface showed that an increasing amplitude and a decreasing wavelength lead to a decrease in stiffness. By increasing the wavelength of the sinusoidal function, an increasing scatter range resulting from the phase shift of the two opposed hinge sides has been identified. Combining the results of waviness and periodic roughness for measured specimens' parameters leads to a maximum deviation of approximately 17.5 % from the ideal stiffness. A variation in the shape parameters of the flexure hinge showed that smaller hinge thicknesses increase the influence of higher-order form deviations. In future work, the investigations will be extended to several hinge contours and compared to measured specimens.

Keywords: compliant mechanism, flexure hinge, bending stiffness, finite element method, surface topography, geometric deviations

1. Introduction

In precision force measurement devices, the kinematic structure is often implemented as a compliant mechanism with concentrated compliances [1-3]. Advantageous properties are zero backlash of the mechanism, highest reproducibility of the motion, a highly accurate motion behavior, and an extreme sensitivity in a dedicated direction due to the low bending stiffness. The latter is achieved by reducing the hinge thickness of the frequently used semi-circular flexure hinges (Figure 1) down to the technologically feasible minimum of about 50 μm [4]. However, prototypes showed crucial differences in the calculated stiffness values driven by manufacturing-related form deviations [5, 6]. Investigations of dimensional deviations were already carried out in the state of the art [7, 8]. The results reveal that the bending stiffness C_ϕ of a semi-circular flexure hinge has the highest sensitivity to the deviation of the thickness t . Deviations of the radius R and the width w are almost negligible. This can be explained considering the parameter coefficients in the mathematical equation (1) for the stiffness of a single semi-circular flexure hinge [9] and the large relative deviation of the thickness due to the manufacturing at the technological limit.

$$C_\phi = \frac{2 \cdot E \cdot w \cdot t^{2.5}}{9 \pi \cdot \sqrt{R}} \quad (1)$$

Notch surface deviations like waviness or roughness also lead to a non-negligible change of the minimal thicknesses in the

significant region. Since this influence has not been addressed in the state of the art, this work deals with the modeling and simulation of semi-circular flexure hinges with surface waviness and roughness. Initially, a suitable approach for implementing the surface topography is selected. Systematic studies are then carried out to conclude for measured profile parameters.

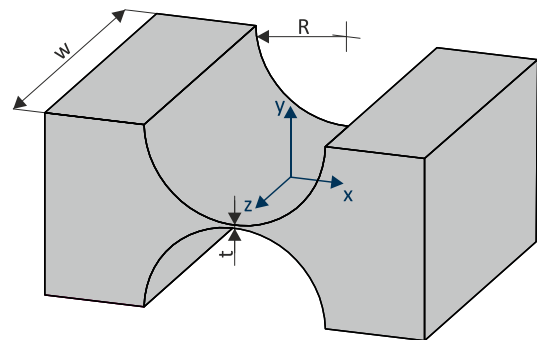


Figure 1. Geometry parameters of the semi-circular flexure hinge.

2. Finite element model of the flexure hinge

The basis for this work is the significant region of a state-of-the-art finite element model of an ideal semi-circular flexure hinge [5]. Its geometric and material parameters are shown in Table 1. The selection of a mathematical approach for manufacturing-related surface deviations and the adaptation and optimization of existing solutions for surface modeling [11, 12] enable the development of a suitable tool.

Table 1. Geometry and material parameters of the ideal flexure hinge.

Parameter	Symbol	Value	Unit
Thickness	t	50	μm
Radius	R	3	mm
Width	w	10	mm
Young's modulus	E	71	GPa
Poisson's ratio	ν	0.33	-

2.1. Mathematical approach for manufactured surfaces

DIN 4760 [10] divides the form deviations into different orders. The effects of dimensional deviations (1st order) on the stiffness can be investigated directly by changing the geometric parameters of the hinge. For deviations of a higher order, a suitable mathematical approach has to be found. Since the waviness (2nd order) and the periodic roughness (3rd order) occur regularly, sine functions according to equation (2) are used.

$$f(x) = a \cdot \sin\left(\frac{2\pi}{\lambda} \cdot x + \phi\right) \quad (2)$$

For this approach, the total height of the waviness Wt and the mean roughness depth Rz are selected as twice the amplitude a . The waviness spacing WSm and the mean peak width RSm define the wavelength λ [13]. The phase shift ϕ is random for both effects. However, the approach is limited by the need to average the locally differing parameters of waviness and periodic roughness.

The form deviations of the 2nd and 3rd order are considered solely along the semi-circular contour. In this case, the modeling of the surface approach leads to a change in the thickness of the hinge over the entire width, to which the stiffness shows the highest sensitivity. Since the significance of the change in thickness for the stiffness decreases with increasing thickness, a high change in stiffness is to be expected due to the heights and depths in the center of the flexure hinge. In the direction of the width, a surface topography according to the approach would lead to neighboring heights and depths in the center. The influences of these heights and depths on the thickness would almost cancel each other out due to a high width-wavelength ratio of at least 40. Thus, the bending stiffness remains nearly unaffected.

4th- and higher-order form deviations are also expected to have a negligible impact on the properties of the flexure hinge since they occur only locally on the surface. The influence on the bending stiffness also decreases the higher the order of the form deviation.

2.2. Characterization of the approach parameter ranges

To specify the definition ranges for the parameters to be investigated, the notch surfaces of five milled semi-circular flexure hinge specimens were characterized using a white light interferometer. The primary profiles were measured ten times per notch across an area of $(250 \times 250) \mu\text{m}^2$ in the direction of the semi-circular contour (Fig. 2 a)). The cut-off wavelength λ_c was set to $25 \mu\text{m}$.

The measured primary profile of each measurement run was filtered and split into the contour with superimposed waviness and roughness (Fig. 2 b)). This enabled an evaluation according to ISO 21920-2 [13] and thus a direct determination of the parameters Wt , WSm , Rz , and RSm intended for the approach. The minima and maxima of all measurements specify the definition ranges (Table 2).

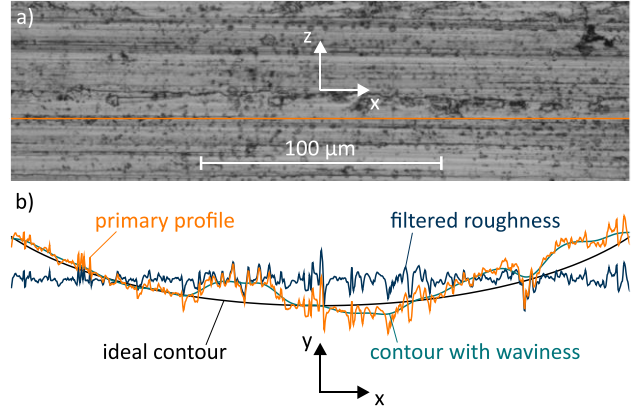


Figure 2. Characterization of the definition ranges of the approach parameters. a) Section of the measured area of the notch surface of a hinge specimen. b) Primary profile of the surface section and application of filters to determine the profile parameters.

Table 2. Ranges of the notch surface profile parameters for $\lambda_c = 25 \mu\text{m}$.

Parameter	Symbol	Minimum	Maximum	Unit
Total height of the waviness	Wt	2.39	7.24	μm
Waviness spacing	WSm	20.00	225.02	μm
Mean roughness depth	Rz	0.67	4.37	μm
Mean peak width	RSm	3.62	8.49	μm

2.3. Setup of the finite element model

The state-of-the-art significant region finite element model of the semi-circular flexure hinge [5] is to be enhanced to integrate manufactured notch surfaces according to the approach described in Chapter 2.1 for the profile parameter ranges defined in Chapter 2.2. However, existing concepts for generating the surface topography [11, 12] proved to be inappropriate, as fine meshing along the semi-circular contour is required. For this, the nodes of the ideal hinge are not moved to implement the surface topography. They are set directly to the intended position during the buildup of the model. The desired position p for each node is determined mathematically using equation (3) for the x-coordinate and equation (4) for the y-coordinate. It depends on the notch surface side, the radius R of the flexure hinge, and the angular position α on the contour.

To ensure consistent meshing of the model, the sections between the surfaces are each divided into elements of equal length. Single nodes, which are connected to the significant region model, are located at both ends. One of these nodes has a degree of freedom of 0 and defines the frame. At the other node, a rotation of $\alpha = 1^\circ$ is initiated and the required moment is evaluated.

$$p_{x,i}(\alpha, r) = \left(r + a \cdot \sin\left(\frac{2\pi}{\lambda} \cdot r \cdot \alpha + \phi\right) \right) \cdot \cos(\alpha) \quad (3)$$

$$p_{y,i}(\alpha, r) = \left(r + a \cdot \sin\left(\frac{2\pi}{\lambda} \cdot r \cdot \alpha + \phi\right) \right) \cdot \sin(\alpha) \pm \left(r + \frac{t}{2} \right) \quad (4)$$

The optimum between realizable profile parameter ranges and computing time was then determined by performing a mesh convergence analysis. For the final model (Figure 3), amplitudes of a maximum of $5 \mu\text{m}$ and wavelengths of at least $100 \mu\text{m}$ can be investigated.

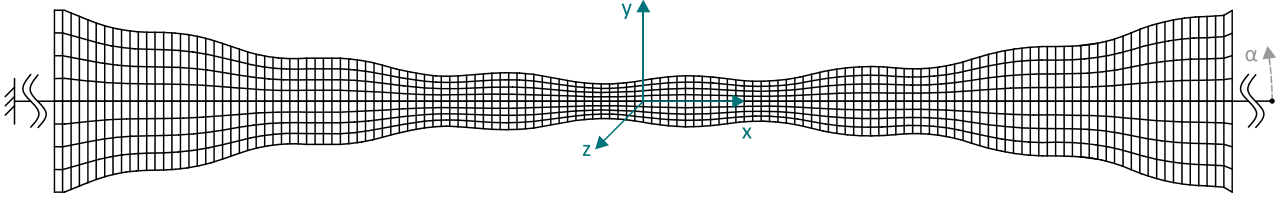


Figure 3. Significant region finite element model of the flexure hinge with manufactured notch surfaces.

3. Stiffness sensitivity to the approach parameters

Due to the wavelength limitation of the model, it is not possible to implement the total definition ranges of the waviness spacing and the mean peak width. For this reason, the investigations are initially carried out using the general approach from equation (2). The definition ranges for the approach parameters are derived from the measured profile parameters ranges from Table 2 (Table 3). In the overall assessment, conclusions for the measured specimen will be drawn.

When developing the design of experiments, it is determined that the amplitude a can be considered individually, as it is a pre-factor of the sine function. The relation between wavelength and phase shift is still unknown. For this reason, they are considered in combination.

Table 3. Definition ranges of the approach parameters.

Parameter	Symbol	Minimum	Maximum	Step size
Amplitude	a	0 μm	5 μm	0.5 μm
Wavelength	λ	100 μm	300 μm	50 μm
Phase shift	ϕ	0	2π	$\pi/4$

3.1. Amplitude

By setting the amplitude to zero, the stiffness of the ideal flexure hinge was determined in the first step. It amounts to $C_{\phi,0} = 18.23 \text{ N mm/rad}$. To investigate the impact of the superimposed amplitude, the phase shift of the sine functions of both surfaces was set to a constant value of zero. Simulation runs were carried out to determine the stiffness $C_{\phi,i}$ of the flexure hinge in dependency of the amplitude for different wavelengths.

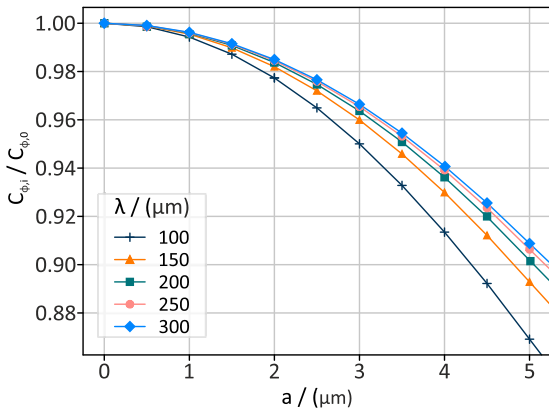


Figure 4. Stiffness amplitude diagram for different wavelengths with the phase shifts set to a constant value of zero.

The stiffness amplitude diagram (Figure 4) reveals first of all that 2nd- and 3rd-order form deviations are always leading to a reduction in stiffness. The stiffness decreases significantly more for larger amplitudes, in the worst case of up to 13 %. It can also be observed that the sensitivity of the stiffness to the amplitude

depends on the wavelength. The shorter the wavelength, the larger the reduction of the stiffness for each amplitude value.

3.2. Wavelength and phase shift

To characterize the sensitivity of the stiffness to the wavelength and the phase shifts, the wavelength was set initially to a constant value and the phase shifts were varied.

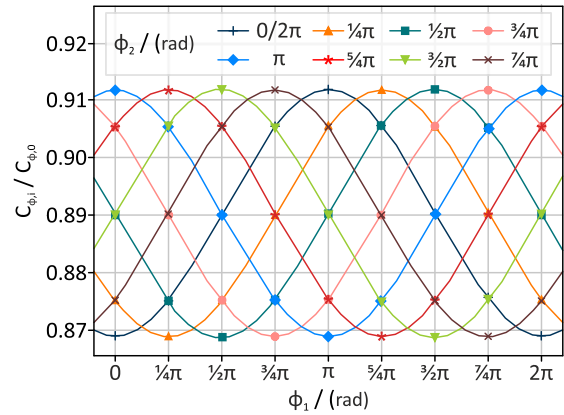


Figure 5. Stiffness phase shift diagram for different phase shifts of the opposite notch surface with a constant wavelength of 100 μm and an amplitude of 5 μm .

The stiffness phase shift diagram for 100 μm wavelength (Figure 5) shows that the phase shifts of the two opposite sides lead to a non-negligible scattering of the stiffness. Contrary to expectations, the maximum stiffness in the scattering area does not occur when the thickness is at its maximum in the middle of the hinge. The maximum is reached when the difference of the phase shifts is a multiple of π . This means the minimum hinge thickness is constant at 50 μm . If both phase shifts have the same value, the stiffness is at its lowest. This is the case for both, the minimum and maximum thickness in the center of the hinge. It becomes clear that not only the center of the hinge is relevant for its stiffness, but the entire significant region.

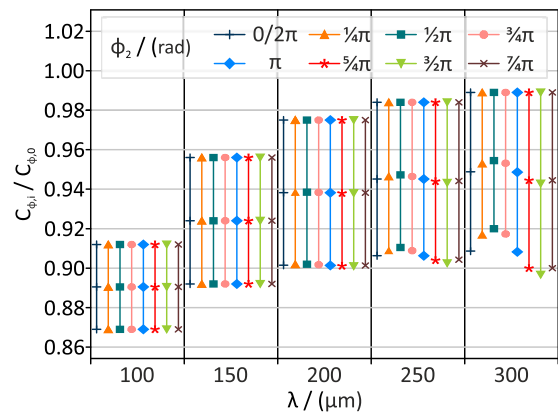


Figure 6. Stiffness scatter ranges resulting from the range of ϕ_1 for different phase shifts ϕ_2 and wavelengths.

Extending the investigations to the entire wavelength range (Figure 6) makes clear that the scatter range increases and the

offset of the mean stiffness decreases with the wavelength. For longer wavelengths, it is also noticeable that the stiffness scattering no longer depends only on the wavelength, but also on the phase shift. To ensure that this effect was not caused by the significant region model, the simulation results were validated for a wavelength of 300 μm with the overall model of the flexure hinge. The occurring variance of the scatter range can be explained by considering the geometric dimensions of the flexure hinge. For longer wavelengths, the material distribution in the stiffness-defining areas around the center of rotation is more asymmetrical compared to shorter wavelengths.

3.3. Surface topography impact for varying geometry

Since higher-order form deviations only occur together with shape deviations (1st order), the influence of the notch surface topography on the stiffness is also considered for a slightly varying geometry. To be able to evaluate the filtered surface impact, the hinge stiffness $C_{\phi,si}$ with notch surface topography was put into relation to the stiffness $C_{\phi,so}$ of the ideal hinge with varied geometric parameters. All investigations were carried out for constant surface parameters with an amplitude of 5 μm , a wavelength of 200 μm , and phase shifts of 0.

The relations between the stiffness change and the change of the geometric parameters (Figure 7) show, that a varying thickness significantly changes the impact of the notch surface topography on the stiffness. In contrast, changing the width and radius has no significant impact.

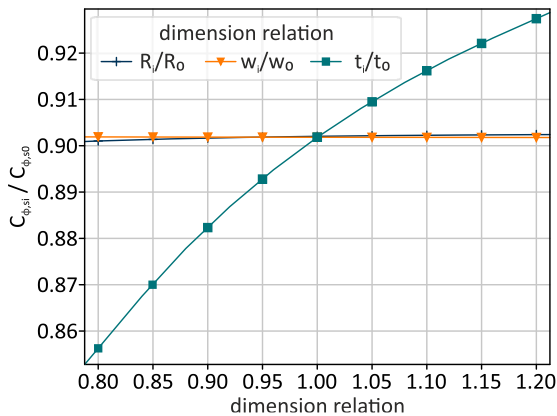


Figure 7. Stiffness dimension change diagram for constant notch surface topography parameters.

4. Conclusions

To be able to evaluate the findings and relate them to the measured specimens, it is necessary to differentiate between the parameters of the approach that can be controlled during manufacturing and those that cannot. The phase shift causing the scatter range of the stiffness is a random value parameter. However, the amplitude and wavelength can be controlled by manufacturing parameters. The amplitude is more critical in terms of stiffness. If the amplitude increases, the stiffness scatter and the mean offset of the stiffness increase. For the wavelength, a distinction must be made. Longer wavelengths lead to a lower mean stiffness offset, but the scattering range of the stiffness is larger. For shorter wavelengths, the effect is reversed. Considering the calculations of the measured specimens (Table 4), it can be seen that the maximum total deviation is almost the same for the measured wavelength range. For shorter wavelengths, however, the scattering range is only half as large. Although the mean stiffness deviation is larger in this case, it can be taken into account during the development of a mechanism or corrected by an oversizing of the hinge

thickness. For the periodic roughness, a large average peak width should be aimed for. The reason is that the scatter range hardly changes and the total offset can therefore be reduced.

Overall, the maximum deviation with the measured profile parameters compared to the ideal hinge is approximately 17.5 %. However, it should be noted that additionally occurring 1st-order form deviations can significantly increase this value.

Table 4. Estimated stiffness deviation for the maximum amplitude in the measured wavelength ranges of the waviness and periodic roughness.

	Wavelength	Mean stiffness reduction	Stiffness scattering
Waviness	20.00 μm	9.01 %	2.03 %
	225.02 μm	6.98 %	4.08 %
Roughness	3.62 μm	7.20 %	0.41 %
	8.49 μm	6.73 %	0.43 %
Combined maxima		16.21 %	4.51 %

5. Outlook

In future work, a calculation model is to be developed to characterize the overall stiffness scatter range of a semi-circular bending hinge, taking into account manufacturing-related form deviations of 1st to 3rd order. This will improve the development of compliant mechanisms. The need to integrate adjustment devices to achieve the desired properties can also be predicted more accurately based on this. The investigations of this work will also be done for other hinge contours. All the obtained results will then be compared to measured hinge prototypes.

Acknowledgment

The authors gratefully acknowledge the support of the Deutsche Forschungsgemeinschaft (DFG) for the financial support of the project with Grant No.: TH845/7-2 and FR2779/6-2 in the framework of the Research Training Group "Tip- and laser-based 3D-Nanofabrication in extended macroscopic working areas" (GRK 2182) at the Technische Universität Ilmenau, Germany.

References

- [1] Darnieder M, Wittke M, Pabst M, Fröhlich T, Theska R 2023 *Engineering for a changing world: 60th ISC, Ilmenau Scientific Colloquium* Article 1.4.112
- [2] Wittke M, Torres Melgarejo M A, Darnieder M, Theska R 2023 *Engineering for a changing world: 60th ISC, Ilmenau Scientific Colloquium* Article 1.3.017
- [3] Keck L, Seifert F, Newell D, Schlamminger S, Theska R, Haddad D 2022 *EPI Techniques and Instrumentation* 9 Article 7
- [4] Bacher J P, Joseph C, Clavel R 2002 *Ind. Robot* 29 349–353
- [5] Torres Melgarejo M A, Darnieder M, Linß S, Zentner L, Theska R 2018 *Actuators* 7 (4) 86
- [6] Darnieder M, Harfensteller F, Schorr P, Scharff M, Linß S, Theska R 2020 *Microactuators, Microsensors and Micromechanisms* 15-24
- [7] Ryu J W, Gweon D-G 1997 *Precision Engineering* 21 (2-3) 83-89
- [8] Shen J Y 2013 *Applied Mechanics and Materials* 302 343-346
- [9] Paros J, Weisbord L 1965 *Machine Design* 25 151–156
- [10] Deutsches Institut für Normung 1982 DIN 4760 – Gestaltabweichungen; Begriffe, Ordnungssystem
- [11] Thompson M K 2006 *Methods for Generating Rough Surfaces in ANSYS International ANSYS Users Conference & Exhibition*
- [12] Wittke M, Melgarejo M A, Darnieder M, Theska R *Proceedings of the 23rd International Conference EUSPEN Copenhagen* 71-72
- [13] International Organization for Standardization 2021 ISO 21920-2 – Geometrical Product Specifications (GPS)